

# Truth Models for Articulating Flexible Multibody Dynamic Systems

Theodore G. Mordfin\*

*CSC Advanced Marine, Arlington, Virginia 22202*

and

Sivakumar S. K. Tadikonda†

*The Catholic University of America, Washington, D.C. 20064*

**Closed-form solutions are developed for the small elastic motions of planar, flexible, multilink systems arranged in chain topologies, in which the links are represented as Euler–Bernoulli bars in transverse vibration. The links are connected by pin joints, the reference articulation angle between adjacent links can be arbitrarily selected, and the system end conditions are set as either pinned or free. The characteristics of the solutions are investigated and are shown to consist of combinations of the characteristic expressions associated with classical end conditions for single links. These solutions are generalized to represent  $n$  links. A large-articulation flexible multibody model of a two-link planar manipulator is then developed and linearized about an arbitrary reference angle configuration. One of the closed-form solutions serves as a truth model in the numerical and analytical evaluation of the use of various types of assumed modes in conjunction with the linearized multibody model. The results further confirm the validity of previously proposed guidelines for selecting assumed modes in articulating flexible multibody systems.**

## Introduction

**S**UBSTRUCTURE synthesis of complex structural dynamics models has a long and successful history in the field of structural dynamics. A number of popular techniques were developed a generation ago<sup>1–5</sup> and have been extensively used ever since. These methods use approximating techniques to represent the small elastic motions of the component substructures. Subsequent research generalized these techniques,<sup>6</sup> described,<sup>7</sup> explained,<sup>7,8</sup> and quantified<sup>9</sup> their convergence properties.

The modeling of flexible component bodies in articulating flexible multibody systems also typically relies on approximating techniques to represent the small elastic motions of the component bodies. However, the subject of robust techniques for modeling component bodies has not been satisfactorily addressed. Lacking clear guidance, applications engineers tend to experience considerable difficulty in developing component-flexible-body model inputs for articulating flexible multibody dynamics simulation software.

Tadikonda et al.<sup>10</sup> rigorously analyzed models for articulating flexible multibody systems from a nonlinear multibody dynamics perspective and developed clear guidelines for modeling the constituent flexible bodies. The effort was necessitated by the numerical difficulties experienced by the authors while modeling the articulated space station and the shuttle remote manipulator systems. Other investigators have reported similar numerical behavior.<sup>11,12</sup> Use of the modeling guidelines developed in Ref. 10 ensures fast convergence of synthesized models, avoidance of unnecessarily high characteristic system frequencies, and maintenance of well-conditioned system mass matrices.

In this paper we analyze articulating flexible multibody systems from a linear structural dynamics perspective and, using closed-form solutions as linear truth models, further test the effectiveness of those modeling guidelines that determine the selection of component body boundary conditions. We begin by examining a two-flexible-link system having an intermediate pin joint, whose inboard link is connected to ground by a pin joint at one end and whose outboard link is free to move at the other end. We derive the equations

of motion for small elastic motions and small articulations about an arbitrary reference angle. We then formulate the corresponding eigenvalue problem and identify the salient features of the system as described by the characteristic equation. We extend the derivation to two-link free-free and two-link pinned-pinned systems, each having an intermediate pinned joint. We then generalize these results to  $n$ -link systems.

Finally, we compare the identified characteristics of the two-flexible-link pinned-free linear truth model to those of a two-flexible-link pinned-free linearized articulated model. In particular, we focus on the guidelines proposed in Ref. 10 for using the assumed modes method in conjunction with an articulating flexible multibody dynamics formulation.<sup>13</sup> The results provide clear insight into the dynamic behavior of the articulating links, from the perspectives of both structural dynamics and articulating flexible multibody dynamics.

As is customary in the literature,<sup>10,13</sup> the term “articulating,” as in articulating joint, indicates large-angle rigid-body motion. However, when discussing closed-form solutions for the dynamic response of the structural systems, the term articulating herein denotes small-angle rotations about pinned joints. The validity of these rotations is limited to the small motions about any arbitrary reference configuration, which can be described by a linear model. The higher-order coupling between the rigid-body motion across articulated joints and the elastic motions of the links is neglected. Accordingly, the characteristic equations associated with the closed-form solutions represent truth models for evaluating both the behavior and linear characteristics of slowly articulating flexible multibody systems. However, these equations also represent truth models for evaluating the characteristics of nonlinear, large-articulation flexible multibody dynamics systems in selected operating configurations. These characteristics provide clear insight to the behavior of such systems and to the selection of assumed modes for representing their material deformations. When simulating rapidly articulating systems that undergo centrifugal stiffening, the guidelines tested and confirmed here represent necessary, but not sufficient, modeling requirements. Additional requirements, discussed in Refs. 10 and 14, also need to be satisfied.

## Two-Link Pinned-Free System

### Kinematics

Consider a two-link, pinned-free system, with arbitrary articulation angles, as shown in Fig. 1. The first link is pinned to ground, and the second link is pinned to the outboard end of the first link.

Received 18 July 1996; revision received 4 September 1999; accepted for publication 17 November 1999. Copyright © 2000 by Theodore G. Mordfin and Sivakumar S. K. Tadikonda. Published by the American Institute of Aeronautics and Astronautics, Inc., with permission.

\*Manager, System Modeling Directorate; also Ph.D. Candidate, Catholic University of America, Washington, DC 20064. Member AIAA.

†Adjunct Assistant Professor; also Senior Principal Engineer, QSS Group, Inc., Seabrook, MD 20706. Senior Member AIAA.

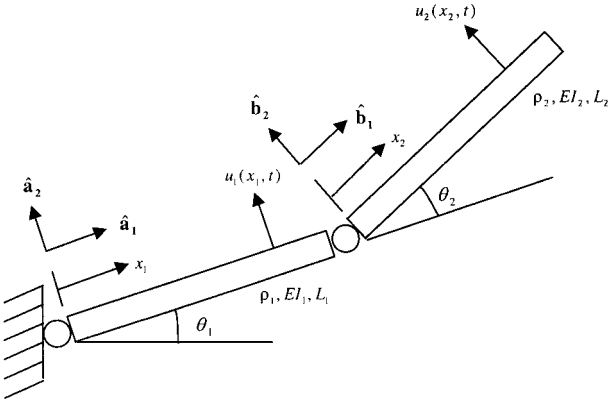


Fig. 1 Two-link, pinned-free system.

The outboard end of the second link is free. The links articulate and bend in the plane of the page. Although such a system is free to undergo large articulations, we assume here that the articulations with respect to any selected reference configuration are very small and restrict the development to a linear system.

We begin by defining the following quantities:  $L_i$  = axial length,  $u_i$  = displacement perpendicular to the bar's axis for link  $i$ ,  $r$  = rigid-body displacement of link 2 along its axis,  $\theta_2$  = rigid-body articulation angle of link 2 with respect to link 1,  $t$  = time, and  $i = 1, 2$ .

Reference frame  $\mathbf{a}$  is fixed to the inboard link, and reference frame  $\mathbf{b}$  is fixed to the outboard link. The joint between the two links is located at point  $p$  on the inboard link and point  $q$  on the outboard link. The location vectors of points  $p$  and  $q$  can be expressed as

$$\mathbf{r}_p = L_1 \hat{\mathbf{a}}_1 + u_1(L_1, t) \hat{\mathbf{a}}_2 \quad (1a)$$

$$\mathbf{r}_q = L_1 \hat{\mathbf{a}}_1 + r(t) \hat{\mathbf{b}}_1 + u_2(0, t) \hat{\mathbf{b}}_2 \quad (1b)$$

where  $\hat{\mathbf{a}}_j$  and  $\hat{\mathbf{b}}_j$  are orthogonal unit vectors fixed in frames  $\mathbf{a}$  and  $\mathbf{b}$ , respectively and  $j = 1, \dots, 3$ . Using these definitions, we express the following holonomic constraint vector:

$$\mathbf{r}_p - \mathbf{r}_q = u_1(L_1, t) \hat{\mathbf{a}}_2 - r(t) \hat{\mathbf{b}}_1 - u_2(0, t) \hat{\mathbf{b}}_2 = 0 \quad (2)$$

which yields the following two scalar constraint equations:

$$\phi_1 = r(t) \cos \theta_2 - u_2(0, t) \sin \theta_2 = 0 \quad (3a)$$

$$\phi_2 = r(t) \sin \theta_2 + u_2(0, t) \cos \theta_2 - u_1(L_1, t) = 0 \quad (3b)$$

### Dynamics

We now define the following additional quantities:  $\rho_i$  = mass per unit length,  $EI_i$  = flexural rigidity,  $dx_i$  = differential length along the bar's axis,  $x_i$  = location along the bar's axis,  $0 \leq x_i \leq L_i$ , and  $i = 1, 2$ . Without loss of generality, we assume uniform stiffness and mass properties over the length of each link. The kinetic energy  $T(t)$ , potential energy  $V(t)$ , and instantaneous work of the workless constraints  $\delta W_c(t)$  for the system can be expressed as

$$T(t) = \frac{1}{2} \int_0^{L_1} \rho_1 \dot{u}_1^2(x_1, t) dx_1 + \frac{1}{2} \int_0^{L_2} \rho_2 \dot{u}_2^2(x_2, t) dx_2 + \frac{1}{2} \int_0^{L_2} \rho_2 \dot{r}^2(t) dx_2 \quad (4)$$

$$V(t) = \frac{1}{2} \int_0^{L_1} EI_1 u_1''^2(x_1, t) dx_1 + \frac{1}{2} \int_0^{L_2} EI_2 u_2''^2(x_2, t) dx_2 \quad (5)$$

$$\delta W_c(t) = \lambda_1 [\cos \theta_2 \delta r(t) - \sin \theta_2 \delta u_2(0, t)] + \lambda_2 [\sin \theta_2 \delta r(t) + \cos \theta_2 \delta u_2(0, t) - \delta u_1(L_1, t)] \quad (6)$$

where  $\lambda_1$  and  $\lambda_2$  are Lagrange multipliers and  $\delta$  is the variational operator. A dot over a variable denotes differentiation with respect

to time, whereas a prime sign represents differentiation with respect to the spatial variable  $x$ .

Applying the extended Hamilton's principle for a constrained system,

$$\int_{t_1}^{t_2} [\delta T(t) - \delta V(t) + \delta W_c(t)] dt = 0 \quad (7)$$

to the system that is represented by Eqs. (4)–(6), and subject to Eqs. (3a) and (3b), we integrate the appropriate terms by parts, eliminate the unknown multipliers, and obtain the following boundary-value problem:

$$\rho_1 \ddot{u}_1 + EI_1 u_1'''' = 0 \quad (8a)$$

$$\rho_2 \ddot{u}_2 + EI_2 u_2'''' = 0 \quad (8b)$$

$$u_1(0, t) = 0 \quad (9a)$$

$$EI_1 u_1''(0, t) = 0 \quad (9b)$$

$$EI_1 u_1''(L_1, t) = 0 \quad (9c)$$

$$u_1(L_1, t) \cos \theta_2 - u_2(0, t) = 0 \quad (9d)$$

$$EI_1 u_1'''(L_1, t) - m_2 \ddot{u}_1(L_1, t) \sin^2 \theta_2 - EI_2 u_2'''(0, t) \cos \theta_2 = 0 \quad (9e)$$

$$EI_2 u_2''(0, t) = 0 \quad (9f)$$

$$EI_2 u_2''(L_2, t) = 0 \quad (9g)$$

$$EI_2 u_2'''(L_2, t) = 0 \quad (9h)$$

Both  $x_1$  and  $x_2$  are measured along the undeformed beam axes, which are arbitrarily oriented, and

$$m_2 = \int_0^{L_2} \rho_2 dx_2$$

Using the method of separation of variables and an assumption of synchronous motion,

$$u_i(x_i, t) = U_i(x_i) e^{j\omega t} \quad (10)$$

in the preceding, we obtain the following eigenvalue problem:

$$U_1''''(x_1) - \beta_1^4 U_1(x_1) = 0 \quad (11a)$$

$$U_2''''(x_2) - \beta_2^4 U_2(x_2) = 0 \quad (11b)$$

subject to the following boundary conditions:

$$U_1(0) = 0 \quad (12a)$$

$$U_1''(0) = 0 \quad (12b)$$

$$U_1''(L_1) = 0 \quad (12c)$$

$$U_1(L_1) \cos \theta_2 - U_2(0) = 0 \quad (12d)$$

$$EI_1 U_1'''(L_1) + m_2 \omega^2 U_1(L_1) \sin^2 \theta_2 - EI_2 U_2'''(0) \cos \theta_2 = 0 \quad (12e)$$

$$U_2''(0) = 0 \quad (12f)$$

$$U_2''(L_2) = 0 \quad (12g)$$

$$U_2'''(L_2) = 0 \quad (12h)$$

where

$$\beta_i^4 = \rho_i \omega^2 / EI_i \quad (13)$$

The solution to the eigenvalue problem has the form

$$U_i(x_i) = A_i \cos(\beta_i x_i) + B_i \sin(\beta_i x_i) + C_i \cosh(\beta_i x_i) + D_i \sinh(\beta_i x_i) \quad (14)$$

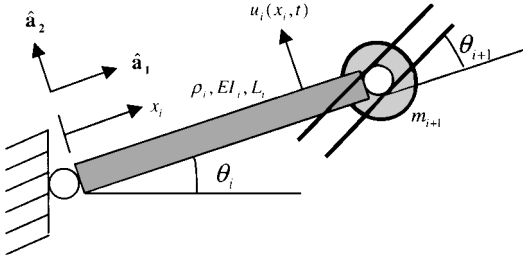


Fig. 2 Pinned/slider-mass beam.

By substituting Eq. (14) in Eqs. (12a–12h), we can derive the system's characteristic equation as

$$EI_1 \beta_1^3 \frac{s_1 ch_1 - c_1 sh_1}{s_1 sh_1} + 2m_2 \omega^2 \sin^2 \theta_2$$

$$= -2EI_2 \beta_2^3 \frac{1 - c_2 ch_2}{s_2 ch_2 - c_2 sh_2} \cos^2 \theta_2 \quad (15)$$

where

$$c_i = \cos(\beta_i L_i), \quad s_i = \sin(\beta_i L_i), \quad ch_i = \cosh(\beta_i L_i)$$

$$sh_i = \sinh(\beta_i L_i), \quad i = 1, 2$$

We recognize the constituent expressions in Eq. (15) as being of three types, and label them as follows:

$$PP_i = \sin(\beta_i L_i) \sinh(\beta_i L_i) \quad (16)$$

which is the characteristic expression of a single pinned-pinned link multiplied by a hyperbolic sine function

$$PF_i = \sin(\beta_i L_i) \cosh(\beta_i L_i) - \cos(\beta_i L_i) \sinh(\beta_i L_i) \quad (17)$$

which is the characteristic expression of a single pinned-free, or free-pinned, bar in bending and

$$FF_i = 1 - \cos(\beta_i L_i) \cosh(\beta_i L_i) \quad (18)$$

which is the characteristic expression of a single free-free link. In the current application none of Eqs. (16–18) is equal to zero.

Substituting Eqs. (16–18) into Eq. (15), we can rewrite the characteristic equation as

$$\frac{Q_1 PF_1 + 2m_2 \omega^2 PP_1 \sin^2 \theta_2}{PP_1} + 2Q_2 \frac{FF_2}{PF_2} \cos^2 \theta_2 = 0 \quad (19)$$

where  $Q_1 = EI_1 \beta_1^3$  and  $Q_2 = EI_2 \beta_2^3$ . We can further simplify the equation by introducing the following composite characteristic expression:

$$PS_i M(\theta_{i+1}) = Q_i PF_i + 2m_{i+1} \omega^2 PP_i \sin^2 \theta_{i+1} \quad (20)$$

which is the characteristic expression of a pinned/slider-mass beam. As shown in Fig. 2, this is a beam that is pinned to ground on its inboard end and loaded on its outboard end by a mass that freely slides in a rotating slot. The slot is free to rotate about the outboard end of the beam. Introducing Eq. (20) into Eq. (19) yields

$$\frac{PS_i M(\theta_2)}{PP_1} + 2Q_2 \frac{FF_2}{PF_2} \cos^2 \theta_2 = 0 \quad (21)$$

Alternatively, we can introduce a different expression

$$SF_i(\theta_i) = Q_i FF_i \cos^2 \theta_i + m_i \omega^2 PF_i \sin^2 \theta_i \quad (22)$$

which is the characteristic expression of a slider-free beam. As shown in Fig. 3, this is a beam that is connected to a slot on its inboard end and is free on its outboard end. The inboard end of the beam is free to both translate and rotate within the slot. Introducing this expression in Eq. (19) and rearranging yields

$$Q_1 \frac{PF_1}{PP_1} + 2 \frac{SF_2(\theta_2)}{PF_2} = 0 \quad (23)$$

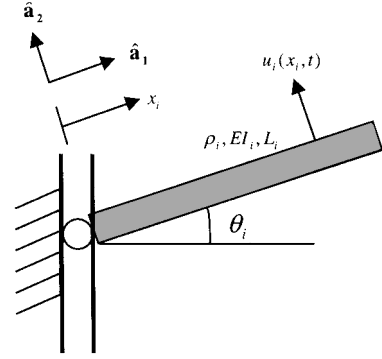


Fig. 3 Slider/free beam.

We can now make the following observations:

1) When  $\theta_2 = 0$  or  $\pi$ , Eq. (19) reduces to

$$Q_1 (PF_1 / PP_1) + 2Q_2 (FF_2 / PF_2) = 0 \quad (24)$$

which shows that the rigid-body mass of the outboard link does not explicitly appear in the collinear case.

2) When  $\theta_2 = \pm \pi/2$ , Eq. (19) reduces to

$$[Q_1 (PF_1 / PP_1) + 2m_2 \omega^2] PF_2 = 0 \quad (25)$$

This equation is satisfied if either of the factors vanishes, and therefore

$$Q_1 (PF_1 / PP_1) + 2m_2 \omega^2 = 0 \quad (26a)$$

and

$$PF_2 = 0 \quad (26b)$$

Equation (26a) is that of a beam pinned at one end and mass loaded at the other end,<sup>15</sup> whereas Eq. (26b) is that of a beam pinned at one end and free at the other. As  $\theta_2$  varies, therefore, the vibrational characteristics of the system vary. Specifically, the bending behaviors of Links 1 and 2 are highly coupled when  $\theta_2 = 0$ , but are entirely decoupled when  $\theta_2 = \pi/2$ . Conversely, the mass loading effect of the outboard beam on the inboard beam reaches its maximum value when  $\theta_2 = \pi/2$ .

3) The characteristics of the links are not those of simple classical bars, but rather are combinations of expressions reminiscent of the characteristics of simple classical bars. In other words, none of the constituent characteristic expressions is equal to zero. This is because the inboard link, Link 1, is more restrained than a pinned-free link, but less constrained than a pinned-pinned link. Similarly, the outboard link, Link 2, is more restrained than a free-free link, but less constrained than a pinned-free link. The only exception to this observation occurs when  $\theta_2 = \pi/2$ , when the system reduces to two uncoupled classical bars. In the case of three or more links, there is no configuration that completely decouples this way.

4) The forms of Eqs. (21) and (23) strongly resemble that of Eq. (24). The pinned-free expression in Eq. (24) is replaced in Eq. (21) by a pinned/slider-mass expression, and one of the free-free expressions in Eq. (24) is replaced in Eq. (23) by a slider/free expression. These observations suggest that the equations can be presented in a recursive form. This subject is addressed in the next section.

Figures 4 and 5 depict a two-link free-free and a two-link pinned-pinned system, respectively. Their characteristic equations can be similarly developed. For a two-link free-free system the equation is

$$\frac{Q_1 FF_1 + m_2 \omega^2 PP_1 \sin^2 \theta_2}{PP_1} + Q_2 \frac{FF_2}{PF_2} \cos^2 \theta_2 = 0 \quad (27)$$

and for a pinned-pinned system it is

$$\frac{Q_1 PF_1 + 2m_2 \omega^2 PP_1 \sin^2 \theta_2}{PP_1} + Q_2 \frac{PF_2}{PP_2} \cos^2 \theta_2 = 0 \quad (28)$$

We define the following intermediate expression:

$$FS_i M(\theta_{i+1}) = Q_i FF_i + m_{i+1} \omega^2 PF_i \sin^2 \theta_{i+1} \quad (29)$$

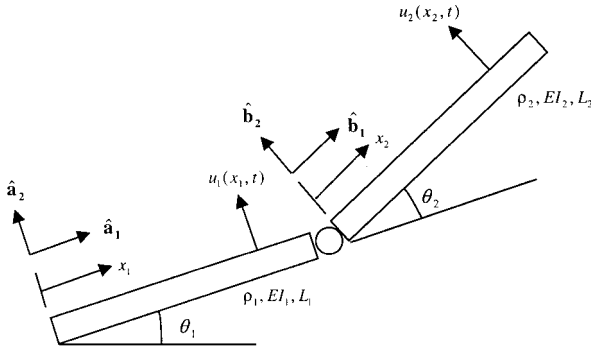


Fig. 4 Two-link, free-free system.

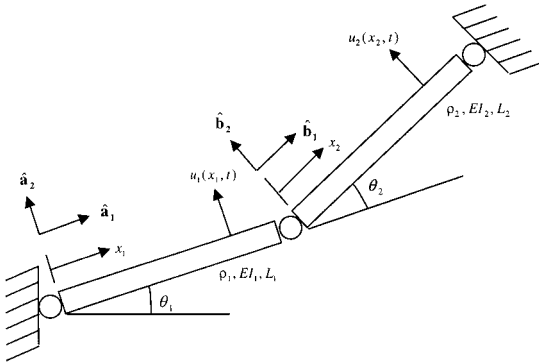


Fig. 5 Two-link, pinned-pinned system.

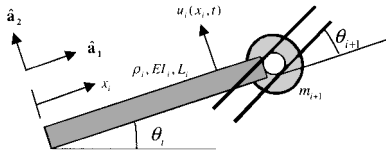


Fig. 6 Free/slider-mass beam.

which is the characteristic expression of a free/slider-mass beam. As shown in Fig. 6, this is a free-free beam, which is loaded on its outboard end by a mass that freely slides in a rotating slot. Recalling Eq. (20), we can express Eqs. (19), (27), and (28), respectively, as

$$2l\_PF(\theta_2) = [PS_1 M(\theta_2)]PF_2 + 2Q_2 PP_1 FF_2 \cos^2 \theta_2 = 0 \quad (30)$$

for the two-link pinned-free system,

$$2l\_FF(\theta_2) = [FS_1 M(\theta_2)]PF_2 + Q_2 PF_1 FF_2 \cos^2 \theta_2 = 0 \quad (31)$$

for the two-link free-free system, and

$$2l\_PP(\theta_2) = [PS_1 M(\theta_2)]PP_2 + Q_2 PP_1 PF_2 \cos^2 \theta_2 = 0 \quad (32)$$

for the two-link pinned-pinned system.

### Three-Link and N-Link Systems

Figure 7 shows a three-link, pinned-free system with arbitrary articulation angles. Proceeding as in the preceding section and assuming small articulations about any selected reference configuration, we can obtain the characteristic equation as

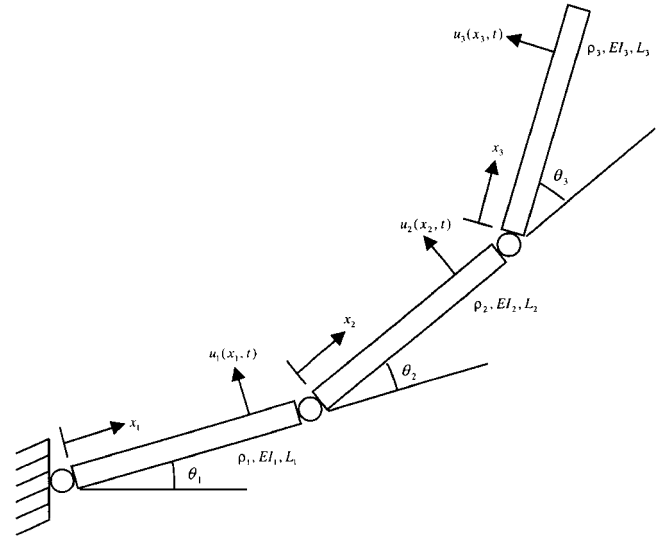


Fig. 7 Three-link, pinned-free system.

Recognizing the constituent characteristic expressions, we simplify the equation to

$$\left\{ \frac{[PS_1 M(\theta_2)][PS_2 M(\theta_3)] + 2Q_2 PP_1 [FS_2 M(\theta_3)] \cos^2 \theta_2}{[PS_1 M(\theta_2)]PP_2 + Q_2 (PP_1)(PF_2) \cos^2 \theta_2} \right\} = -2Q_3 \left( \frac{FF_3}{PF_3} \right) \cos^2 \theta_3 \quad (34)$$

We then recognize the denominator of the left-hand-side expression as  $2l\_PP(\theta_2)$ . The numerator of the left-hand side is similar in form to a rearranged version of  $2l\_PF(\theta_2)$ , in which the outboard end of the second link is pinned/slider-mass loaded, as shown in Fig. 2, instead of free. Accordingly, we denote this expression as  $2l\_PS_2 M(\theta_3)$  and write the characteristic equation as

$$\frac{2l\_PS_2 M(\theta_3)}{2l\_PP(\theta_2)} = -2Q_3 \frac{FF_3}{PF_3} \cos^2 \theta_3 \quad (35)$$

Comparing the form of this equation to that of Eqs. (19), (21), and (23), it is now quite apparent that the characteristic equation can be written recursively. As a result, we write the equation for an n-link pinned-free system as

$$nl\_PF(\theta) = 2\gamma_{n-1} FF_n \cos^2 \theta_n + PF_n = 0 \quad (36)$$

where

$$\gamma_i = Q_{i+1} \left\{ \frac{\gamma_{i-1} PF_i \cos^2 \theta_i + PP_i}{2\gamma_{i-1} [FS_i M(\theta_{i+1})] \cos^2 \theta_i + [PS_i M(\theta_{i+1})]} \right\} \quad i \geq 1 \quad (37a)$$

$$\gamma_0 = 0 \quad (37b)$$

Similar equations can be written for n-link free-free and pinned-pinned systems. For the n-link free-free system

$$nl\_FF(\theta) = \gamma_{n-1} FF_n \cos^2 \theta_n + PF_n = 0 \quad (38)$$

where

$$\gamma_i = Q_{i+1} \left\{ \frac{PF_i \cos^2 \theta_i + 2PP_i / \gamma_{i-1}}{[FS_i M(\theta_{i+1})] \cos^2 \theta_i + [PS_i M(\theta_{i+1})] / \gamma_{i-1}} \right\} \quad i \geq 1 \quad (39a)$$

$$\gamma_0 = \infty \quad (39b)$$

$$\left\{ \frac{[(Q_1 PF_1 + 2m_2 \omega^2 PP_1 \sin^2 \theta_2) / Q_2 PP_1] (Q_2 PF_2 + 2m_3 \omega^2 PP_2 \sin^2 \theta_3) + 2(Q_2 FF_2 + 2m_3 \omega^2 PF_2 \sin^2 \theta_3) \cos^2 \theta_2}{[(Q_1 PF_1 + 2m_2 \omega^2 PP_1 \sin^2 \theta_2) / Q_2 PP_1] PP_2 + PF_2 \cos^2 \theta_2} \right\} = -2Q_3 \frac{FF_3}{PF_3} \cos^2 \theta_3 \quad (33)$$

and for the n-link pinned-pinned system

$$nL_{PP}(\theta) = \gamma_{n-1}PF_n \cos^2 \theta_n + PP_n = 0 \quad (40)$$

where

$$\gamma_i = Q_{i+1} \left\{ \frac{\gamma_{i-1}PF_i \cos^2 \theta_i + PP_i}{2\gamma_{i-1}[FS_i M(\theta_{i+1})] \cos^2 \theta_i + [PS_i M(\theta_{i+1})]} \right\} \quad i \geq 1 \quad (41a)$$

$$\gamma_0 = 0 \quad (41b)$$

### Implications for Modeling Using Assumed Modes Approach

We now investigate the issue of what type of component-body modes is most appropriate for modeling the links of nonlinear, articulating flexible multibody systems using the assumed modes approach. We accomplish this by linearizing a nonlinear assumed modes system model about an arbitrary configuration and comparing the computed characteristic frequencies of this system with the characteristic frequencies of a linear closed-form solution of the same configuration. We incorporate several types of component-body modes in the linearized assumed modes model and demonstrate what types of assumed modes are most appropriate. The closed-form solution provides both exact characteristic frequencies for comparison and an analytical basis for evaluating the variation of assumed-modes-model accuracy with variations in reference articulation angle. Although Ref. 16 developed closed-form solutions for two-link nonplanar systems, it did not reduce them to concise, recognizable forms and did not analytically evaluate their behavior.

#### Linearized Assumed Modes Model

The system to be tested is the two-link pinned-free system with an intermediate pin joint, which is depicted in Fig. 1 and described in an earlier section. We summarize the development of the linearized assumed modes model as follows. Let  $\phi_{1j}(x_1)$  and  $\phi_{2j}(x_2)$  be the assumed modes and  $\eta_{1j}(t)$  and  $\eta_{2j}(t)$  represent their time-dependent amplitudes for Links 1 and 2, respectively. Link 1 denotes the link that is pinned to the ground. Let  $\theta_1(t)$  denote the angle between the undeformed Link 1 axis and a reference axis attached to the ground, and let  $\theta_2(t)$  denote the angle between the undeformed link axes. The linear and angular momentum coefficients and modal mass terms associated with these mode shapes are defined as<sup>10,17</sup>

$$\alpha_{kj} = \int_0^{L_k} \rho_k \phi_{kj} dx_k, \quad k = 1, 2, \quad j = 1, 2, \dots, N_k \quad (42)$$

$$h_{kj} = \int_0^{L_k} \rho_k x_k \phi_{kj} dx_k, \quad k = 1, 2, \quad j = 1, 2, \dots, N_k \quad (43)$$

$$m_{kij} = \int_0^{L_k} \rho_k \phi_{ki} \phi_{kj} dx_k, \quad k = 1, 2, \quad i, j = 1, 2, \dots, N_k \quad (44)$$

where  $N_1$  and  $N_2$  denote the number of modes used for representing link flexibility. Employing the articulating flexible multibody formulation of Ref. 13 and assuming uniform mass distribution along each link, the zeroth order mass matrix  $M$  for this system can be obtained as

$$M_{11} = \rho_1 L_1^3/3 + \rho_2 L_2 (L_2^2/3 + L_1^2 + L_1 L_2 \cos \theta_2) \quad (45a)$$

$$M_{1,1+j} = h_{1j} + \rho_2 L_2 (L_1 + 0.5 L_2 \cos \theta_2) \phi_{1j}(L_1) \quad j = 1, 2, \dots, N_1 \quad (45b)$$

$$M_{1,2+N_1} = \rho_2 L_2 (L_2^2/3 + 0.5 L_1 L_2 \cos \theta_2) \quad (45c)$$

$$M_{1,2+N_1+j} = h_{2j} + L_1 \alpha_{2j} \cos \theta_2, \quad j = 1, 2, \dots, N_2 \quad (45d)$$

$$M_{1+i,1+j} = m_{1ij} + \rho_2 L_2 \phi_{1i}(L_1) \phi_{1j}(L_1), \quad i, j = 1, 2, \dots, N_1 \quad (45e)$$

$$M_{1+i,1+N_1+j} = \phi_{1i}(L_1) \alpha_{2j} \cos \theta_2 \quad i = 1, 2, \dots, N_1, \quad j = 1, 2, \dots, N_2 \quad (45f)$$

$$M_{2+N_1,2+N_1} = \rho_2 L_2^3/3 \quad (45g)$$

$$M_{2+N_1,1+j} = 0.5 \rho_2 L_2^2 \phi_{1j}(L_1) \cos \theta_2, \quad j = 1, 2, \dots, N_2 \quad (45h)$$

$$M_{2+N_1,2+N_1+j} = h_{2j}, \quad j = 1, 2, \dots, N_2 \quad (45i)$$

$$M_{2+N_1+i,2+N_1+j} = m_{2ij}, \quad i, j = 1, 2, \dots, N_2 \quad (45j)$$

$$M_{ji} = M_{ij}, \quad i, j = 1, 2, \dots, 2 + N_1 + N_2 \quad (45k)$$

The system stiffness matrix  $K$  can be expressed as

$$K_{i+1,j+1} = \int_0^{L_1} EI_1 \phi_{1i}''(x_1) \phi_{1j}''(x_1) dx_1, \quad i, j = 1, 2, \dots, N_1 \quad (46a)$$

$$K_{2+N_1+i,2+N_1+j} = \int_0^{L_1} EI_2 \phi_{2i}''(x_2) \phi_{2j}''(x_2) dx_2 \quad i, j = 1, 2, \dots, N_2 \quad (46b)$$

$$K_{ij} = 0, \quad \text{otherwise} \quad (46c)$$

For slow, small motions about the articulation angles  $\theta_1$  and  $\theta_2$ , high-order coupling between states can be neglected. Therefore, the system equations of motion can be linearized and expressed as

$$M\ddot{q} + Kq = 0 \quad (47)$$

where  $q = [\theta_1 \eta_{11} \eta_{12}, \dots, \eta_{1N_1} \theta_2 \eta_{21} \eta_{22}, \dots, \eta_{2N_2}]^T$ .

Although Eq. (47) represents a linearized system, it contains significant characteristics of the nonlinear system from which it was derived. Specifically, it contains linear expressions for the deformational motions of each component body, the exact rigid-body mass properties, and expressions for the interactions between the rigid-body and deformational motions. These features are fundamental to the synthesized system characteristics, which are investigated next.

#### Test Approach

We can now select a particular set of assumed modes, generate the  $M$  and  $K$  matrices in Eq. (47), and solve for the frequencies of the combined system for any reference articulation angle. Reference 10 recommends imposing the following requirements on the assumed modes used to represent the deformations of each component body:

- 1) The geometric boundary condition imposed at the inboard end of the component-body structural model must be the same as that in the physical system if the boundary were attached to ground.
- 2) Mass-augmented modes must be used to account for the effects of outboard bodies.

Following these recommendations, the inboard link should be modeled using pinned-free/mass-augmented modes, with the mass-augmentation equaling the mass of the outboard body. The outboard link should be modeled using pinned-free modes. Reference 10 tested the recommendations on a single-link system, whose characteristics are independent of articulation angle. We now test the effectiveness of the recommendations for the two-link system at hand for arbitrary reference articulation angles.

In conducting the tests we compare the effectiveness of using fixed-free modes for both links, pinned-free modes for both links, and the recommended modes for each link. All of these choices clearly violate the system characteristic equation. However, in the general case involving complex component bodies, it is impossible to generate assumed modes that satisfy it. Furthermore, practical applications tend to rely on finite element modeling tools in generating the assumed modes. In such cases no attempt is made to analytically develop eigenfunctions. Nevertheless, it is important to understand the ramifications of using various types of assumed modes.

Test Results

Table 1 shows the frequencies obtained by solving the eigenvalue problem related to Eq. (47) with component fixed-free modes, pinned-free modes, and pinned-free/mass augmented modes, when  $\theta_2 = 0$  or  $\pm\pi$ . Table 2 shows the frequencies when  $\theta_2 = \pm\pi/2$ . The component links have unit mass, stiffness, and geometric properties  $\rho_1 = \rho_2 = 1$ ,  $EI_1 = EI_2 = 1$ , and  $L_1 = L_2 = 1$ . Tables 1 and 2 also show the solutions to the characteristic equation, Eq. (30), for the appropriate articulation angles.

We observe that the frequencies of the synthesized system in Eq. (47) best approximate the frequencies of the characteristic equation when the recommended component modes are used for each link. As just stated, these are pinned-free/mass-augmented modes for Link 1 and pinned-free modes for Link 2. These component modes satisfy the geometric boundary conditions while not violating the complementary boundary conditions.<sup>8</sup> In addition, their use minimizes both the coupling of the system mass matrix and its condition number, which suggests that they represent a very appropriate set. Conversely, the frequencies of the synthesized system most poorly approximate the frequencies of the characteristic equation when component fixed-free modes are used for both the links. These modes violate most of the geometric and complementary boundary conditions. In addition, the fixed-free mode set maximizes both the coupling of the mass matrix and its condition number, which suggests that it represents a very inappropriate set. The fixed-free modes also cause the generation of one unnecessarily high-frequency mode per articulating joint. Reference 10 provides an analytical explanation for this phenomenon.

The variation of articulation angles allows us to make the following additional observations:

1) The synthesized systems match the exact frequencies the best when  $\theta_2 = \pm\pi/2$  and the worst when  $\theta_2 = 0$ . It can be easily demonstrated that as the reference articulation angle is varied from 0 or  $\pi$  to  $\pm\pi/2$  the characteristic frequencies decrease monotonically, but not uniformly. At the same time the accuracies of the synthesized models tend to increase because of the decreasing coupling of the governing equations.

2) When  $\theta_2 = \pm\pi/2$ , the frequencies obtained from the assumed modes model, which uses mass augmented modes, exactly equal the exact frequencies. The reason is as follows. From a structural dynamics perspective the modeling assumptions cause the links to decouple in bending, and the links therefore behave as classical pinned-free and pinned/mass-loaded bars. This phenomenon is illustrated by Eq. (25). However, from a multibody dynamics perspective it is clear that the selection of the assumed modes determines whether or not this phenomenon is captured. Whereas all angle-dependent terms in the system mass matrix vanish because  $\cos(\pm\pi/2) = 0$ , the values of many other terms depend on the types of assumed modes selected. When mass-normalized pinned-free/mass-augmented and pinned-free modes are used for Links 1 and 2, respectively, the portions of the modal mass block represented by Eqs. (45e) and (45j) become identity. Coupling between the rigid-body and flexible-body behavior represented by the non-angle-dependent portions of Eqs. (45b), (45d), and (45i) identically vanishes. The resulting mass matrix is diagonal, and the obtained frequencies are the square roots of the diagonal elements of the modal stiffness matrix. As a result, the expansion theorem<sup>18</sup> guarantees that the obtained frequencies will be exact.

3) When  $\theta_2 = \pm\pi/2$ , alternate frequencies obtained from the assumed modes model, which uses pinned-free modes for both links,

Table 1 Comparison of system frequencies synthesized using component modes to system frequencies from characteristic equation;  $EI_1 = 1 = EI_2$ ,  $L_1 = 1 = L_2$ ,  $\rho_1 = 1 = \rho_2$ , and  $\theta_2 = 0$  or  $\pm\pi$

System frequencies obtained by solving the characteristic equation, rad/s	Frequencies (rad/s) obtained from the synthesized system using component modes					
	Link 1:		Link 1:		Link 1:	
	Fixed-free for both links, and $N_1 = N_2 = 3$	Pinned-free for both links, and $N_1 = N_2 = 3$	pinned-mass augmented; Link 2: pinned-free, $N_1 = N_2 = 3$	Fixed-free for both links, and $N_1 = N_2 = 5$	Pinned-free for both links, and $N_1 = N_2 = 5$	pinned-mass augmented; Link 2: pinned-free, $N_1 = N_2 = 5$
11.5140	11.5453	11.5280	11.5142	11.5202	11.5179	11.5140
19.9213	19.9437	19.9356	19.9294	19.9265	19.9248	19.9222
42.8424	43.1694	43.0367	42.8588	42.9178	42.8949	42.8443
57.6327	58.0367	57.8156	57.8461	57.6880	57.6677	57.6553
93.8294	<b>154.1022</b>	94.9359	94.0773	94.4447	94.0919	93.8514
115.2144	<b>197.5372</b>	116.9524	118.6841	115.3726	115.4039	115.4051
164.5620	—	—	—	166.1229	165.4401	164.7014
192.5258	—	—	—	193.7505	193.3366	193.6167
255.0333	—	—	—	<b>436.1855</b>	257.5960	255.8064
289.5769	—	—	—	<b>530.2671</b>	293.7670	298.3681

Table 2 Comparison of system frequencies synthesized using component modes to system frequencies from characteristic equation;  $EI_1 = 1 = EI_2$ ,  $L_1 = 1 = L_2$ ,  $\rho_1 = 1 = \rho_2$ , and  $\theta_2 = \pm\pi/2$

System frequencies obtained by solving the characteristic equation, rad/s	Frequencies (rad/s) obtained from the synthesized system using component modes					
	Link 1:		Link 1:		Link 1:	
	Fixed-free for both links, and $N_1 = N_2 = 3$	Pinned-free for both links, and $N_1 = N_2 = 3$	pinned-mass augmented; Link 2: pinned-free, $N_1 = N_2 = 3$	Fixed-free for both links, and $N_1 = N_2 = 5$	Pinned-free for both links, and $N_1 = N_2 = 5$	pinned-mass augmented; Link 2: pinned-free, $N_1 = N_2 = 5$
10.7144	10.7582	10.7350	10.7144	10.7234	10.7202	10.7144
15.4182	15.4194	15.4182	15.4182	15.4182	15.4182	15.4182
40.3986	40.9037	40.7507	40.3986	40.5358	40.4967	40.3986
49.9649	50.1274	49.9649	49.9649	49.9673	49.9649	49.9649
89.7730	<b>153.3008</b>	91.7904	89.7730	90.7877	90.2910	89.7730
104.2476	<b>162.7676</b>	104.2477	104.2477	104.3415	104.2477	104.2477
158.8735	—	—	—	161.0878	160.6071	158.8736
178.2697	—	—	—	179.2853	178.2697	178.2697
247.7080	—	—	—	<b>435.8218</b>	252.5537	247.7081
272.0309	—	—	—	<b>446.4856</b>	272.0310	272.0310

are exact, whereas the others are in error. The error in this assumed modes model is caused by the lack of mass augmentation in the assumed modes for the inboard link. Because the deformational behaviors of the links are dynamically decoupled, the modes alternately represent the inboard and outboard link behavior. The use of pinned-free modes causes an error for the inboard link, but produces exactly correct results for the outboard link.

### Summary

The test results confirm the validity of the modeling guidelines proposed in Ref. 10. These results demonstrate the necessity and the effectiveness of selecting the recommended boundary conditions when creating component-body structural models for articulating, flexible multibody dynamics systems. The closed-form solutions developed, and the tests conducted against them, are valid for slowly articulating flexible multibody dynamics systems. The guidelines provide a necessary, but not sufficient, set of modeling requirements for rapidly articulating systems that undergo centrifugal stiffening. Models of such systems must also satisfy additional requirements, which are discussed in Refs. 10 and 14.

### Conclusions

Closed-form solutions have been developed for the small elastic motions of three types of planar, flexible, n-link systems arranged in chain topologies, in which the links are connected by pin joints. The solutions are valid for evaluating the behavior and characteristics of linear elastic systems undergoing slow, small articulations about arbitrary reference-angle configurations. However, they are also valid for evaluating the characteristics of large-angle articulating flexible multibody dynamics systems. These characteristics provide clear insight to the behavior of such systems and to the selection of assumed modes for representing their material deformations. Accordingly, one of the closed-form solutions was used as a truth model to evaluate the use of various types of assumed modes in conjunction with a linearized articulating flexible multibody dynamic model of a two-link planar manipulator. Numerical results were presented and evaluated by investigating the analytical forms of both the closed-form solutions and the articulating flexible multibody model. The results of the evaluations further confirm the validity of guidelines already proposed for selecting boundary conditions when creating flexible component-body models. Use of the guidelines ensures fast convergence of synthesized models, avoidance of unnecessarily high characteristic system frequencies, and maintenance of well-conditioned system mass matrices. These guidelines represent necessary, but not always sufficient, requirements for component-body modeling. Models of rapidly articulating systems that undergo centrifugal stiffening must also satisfy additional requirements that are already specified in the open literature.

### Acknowledgments

The first author gratefully acknowledges the support of Nichols Advanced Marine and Peter Peter Zahn, director of its Modeling and Simulation Division, who made possible the execution of part of the work reported herein.

### References

- <sup>1</sup>Hurty, W. C., "Dynamic Analysis of Structural Systems Using Component Modes," *AIAA Journal*, Vol. 3, No. 4, 1965, pp. 678–685.
- <sup>2</sup>Craig, R. R., and Bampton, M. C. C., "Coupling of Substructures for Dynamic Analysis," *AIAA Journal*, Vol. 6, No. 7, 1968, pp. 1313–1319.
- <sup>3</sup>MacNeal, R. H., "A Hybrid Method of Component Mode Synthesis," *Computers and Structures*, Vol. 1, 1971, pp. 581–601.
- <sup>4</sup>Craig, R. R., and Chang, C. J., "On the Use of Attachment Modes in Substructure Coupling for Dynamic Analysis," *AIAA Paper 77-405*, 1977.
- <sup>5</sup>Benfield, W. A., and Hruda, R. F., "Vibration Analysis for Structures by Component Mode Substitution," *AIAA Journal*, Vol. 9, No. 7, 1971, pp. 1255–1261.
- <sup>6</sup>Hale, A. H., and Meirovitch, L., "A General Substructure Synthesis Method for the Dynamic Simulation of Complex Structures," *Journal of Sound and Vibration*, Vol. 69, No. 2, 1980, pp. 309–326.
- <sup>7</sup>Meirovitch, L., and Kwak, M. K., "Rayleigh-Ritz Based Substructure Synthesis for Flexible Multibody Dynamic Systems," *AIAA Journal*, Vol. 29, No. 10, 1991, pp. 1709–1719.
- <sup>8</sup>Baruh, H., and Tadikonda, S. S. K., "Another Look at Admissible Functions," *Journal of Sound and Vibration*, Vol. 132, No. 1, 1989, pp. 73–87.
- <sup>9</sup>Tadikonda, S. S. K., and Baruh, H., "Gibbs Phenomenon in Structural Mechanics," *AIAA Journal*, Vol. 29, No. 9, 1991, pp. 1488–1497.
- <sup>10</sup>Tadikonda, S. S. K., Mordfin, T. G., and Hu, T. G., "Assumed Modes Method and Articulated Flexible Multibody Dynamics," *Journal of Guidance, Control, and Dynamics*, Vol. 18, No. 3, 1995, pp. 404–410.
- <sup>11</sup>Hablani, H. B., "Hinges-Free and Hinges-Locked Modes of a Deformable Multibody Space Station—A Continuum Approach," *Journal of Guidance, Control, and Dynamics*, Vol. 13, No. 2, 1990, pp. 286–296.
- <sup>12</sup>Singh, S. N., and Schy, A. A., "Control of Elastic Robotic Systems by Nonlinear Inversion and Modal Damping," *Journal of Dynamic Systems, Measurement and Control*, Vol. 108, Sept. 1986, pp. 180–189.
- <sup>13</sup>Singh, R. P., VanderVoort, R. J., and Likins, P. W., "Dynamics of Flexible Bodies in Tree Topology—A Computer-Oriented Approach," *Journal of Guidance, Control, and Dynamics*, Vol. 8, No. 5, 1985, pp. 584–590.
- <sup>14</sup>Tadikonda, S. S. K., and Chang, H. T., "On the Geometric Stiffness Matrices in Flexible Multibody Dynamics," *Journal of Vibration and Acoustics*, Vol. 117, Oct. 1995, pp. 452–461.
- <sup>15</sup>Magrab, E. B., *Vibrations of Elastic Structural Members*, Sijhoff and Noordhoff, Alphen aan den Rijn, The Netherlands, 1979.
- <sup>16</sup>Book, W. J., Maizza-Neto, O., and Whitney, D. E., "Feedback Control of Two Beam, Two Joint Systems with Distributed Flexibility," *Journal of Dynamic Systems, Measurement, and Control*, Vol. 101, No. 3, 1979, pp. 187–192.
- <sup>17</sup>Hughes, P. C., "Modal Identities for Elastic Bodies, with Application to Vehicle Dynamics and Control," *Journal of Applied Mechanics*, Vol. 47, March 1980, pp. 177–184.
- <sup>18</sup>Meirovitch, L., *Computational Methods in Structural Dynamics*, Sijhoff and Noordhoff, Alphen aan den Rijn, The Netherlands, 1980.